

Adaptive control scheme of variable speed wind turbines for frequency support

Leonardo Javier Ontiveros, Antonio Ernesto Sarasua, Cindy Madrid-Chirinos

Institute of Electrical Energy (IEE), Faculty of Engineering, National University of San Juan (UNSJ), San Juan, Argentina

Article Info

Article history:

Received Apr 24, 2024

Revised Mar 5, 2025

Accepted May 6, 2025

Keywords:

Adaptive control scheme

Frequency control

Transient response

Virtual synchronous machine

Wind generation

ABSTRACT

Wind generation has experienced significant growth in power systems, due to the high availability of the primary resource and the maturity of its technology, which allows a fast control of active and reactive power. However, its main disadvantage is the lack of controllability over the primary resource. This leads to unwanted frequency oscillations that affect the power system security as wind penetration increases. This is due to the inertia of wind turbines is decoupled from the inertia of synchronous machines connected to the power system. Based on the aforementioned information, this paper analyses the state of the art of control strategies that allow wind turbines to participate in the frequency control of the power system. The main contribution of this work is the novel control strategy proposed, which implements a virtual synchronous machine controlled by an adaptive control system to enhance the transient response of the wind turbine. This scheme allows efficient management of the turbine's rotating reserve without the need to reduce its output power or use expensive energy storage systems. This solution is suitable for power systems with high wind penetration (above 20%). The validity of this proposal is demonstrated through dynamic simulations in a test system.

This is an open access article under the [CC BY-SA](#) license.



Corresponding Author:

Leonardo Ontiveros

Institute of Electrical Energy (IEE), Faculty of Engineering, National University of San Juan (UNSJ)

Av. Libertador 1109 West, San Juan 5400, Argentina

Email: lontiveros@iee-unsjconicet.org

1. INTRODUCTION

The depletion of world fossil fuels reserves and the growing environmental pollution have originated the development of renewable energy sources in recent decades. Currently, renewable energies have been established around the world as an important source of energy. Due to its rapid growth, the energy sector of developing countries is shifting to “energy transition” where renewable energy plays a leading role moving from a conventional scheme based on thermal, and nuclear power plants to an alternative generation scheme.

Within the renewable energy portfolio, wind generation has experienced a considerable growth in recent years, currently it is one of the most attractive alternatives [1], [2]. The advantages are the high availability of the primary resource, the maturity of the technology with increasingly competitive costs, and the connection to the electrical network through electronic power devices allows rapid control of active and reactive power [2], [3]. Among the disadvantages of wind generation include high installation costs and lack of controllability over the primary resource [2]. Depending on a primary energy source that is not easy controllable and under a significant penetration level, wind generation leads to conflicts in the electrical power system. For this reason, electricity companies are forced to evaluate the influence of wind generation on various aspects of the electricity system [4]. Among them, we can highlight the power quality (e.g.,

voltage violations, and/or insufficient reserve of reactive power) and the power system security (e.g., problems associated with the generation reserve due to the impossibility to control the primary energy source). Considering these problems caused by the incorporation of wind generation into the power system, it is necessary to analyze and develop solutions to minimize its impact.

This work evaluates an important aspect of the power system security: the frequency control. Frequency control is seriously affected in systems with a high level of wind penetration (WP). This is due to the inertia of wind turbines (WTs) is decoupled from the inertia of synchronous machines connected to the power system. In the case of WT with a full-scale power converter, the mentioned converter decouples the rotor speed from the system frequency. In this way, when a disturbance occurs, these WTs do not offer an inertial response; therefore, the dynamic response of the power system is less damped than the case when the WP is low. Then, if the WP level continues to increase, the total inertia of the power system reduces, and it is necessary to increase the generation reserve in the electrical system. In WTs, this generation reserve is obtained by reducing their output power, this causes the dispatch of conventional power plants in order to cover the same demand, leading to greater pollution and contradicting the purpose for which they were designed (clean energy). On the other hand, if the generation reserve is not increased and a disturbance occurs, the system presents a reduced inertia value that leads to greater frequency deviations from its nominal value, which can cause the disconnection of the load or even, in extreme cases, the collapse of the electrical system.

Based on the aforementioned information, first this paper analyses the state of the art of control strategies that allow WTs to participate in the frequency control of the power system. Then, a novel control strategy is proposed, which implements a virtual synchronous machine controlled by an adaptive control scheme to enhance the transient response of the WT. This control proposal takes advantage of the kinetic energy stored in the inertia of the rotating mass, thereby obtaining the generation reserve without reducing the output power of the WT. This solution allows increasing WP without the need to increase the generation reserve of conventional generation plants. This alternative is ideal for power systems with high WP (above 20%), characterized by their stochastic, non-linear and time-varying behavior. This is demonstrated by dynamic simulations in a test system.

2. METHOD

Current technological developments enhance the control capabilities of WTs, allowing wind farms to participate in the frequency control of the electrical system and consequently, to improve the power system security. This leads to the revision of the current grid codes by system operators. Nowadays, there are three principles to perform frequency control with wind farms [5], [6]: droop control, damping control, and inertial control. In the droop control, the power of the WT is proportional to the deviation of frequency (Δf), as occurs in conventional generators. Generally, a droop factor (R) between 0.03 and 0.05 pu is used. For example, if the value of R is 0.05, and the actual frequency varies from 1.0 pu to 0.95 pu, the power of the droop control P_{droop} varies from 0 pu to 1.0 pu is (1).

$$P_{droop} = \frac{(f_0 - f)}{R} = \frac{\Delta f}{R} [pu] \quad (1)$$

Where f_0 is the rated frequency (1.0 pu) and f is the actual frequency in pu. Note that P_{droop} is positive when f is less than f_0 .

The damping control calculates a power component P_{damp} that helps to attenuate unwanted oscillations. This term is not always used; generally, it is applied when the system presents an underdamped response or frequency variations caused by renewable generation. In order to calculate the value of P_{damp} , a damping coefficient k_D is employed as (2).

$$P_{damp} = k_D \Delta f = k_D (f_0 - f) [pu] \quad (2)$$

In inertial control, the power generated by the WT is proportional to the derivative of the system frequency. In the strict sense, this component is obtained from the differential equation that describes the dynamic behavior of the WT, given as (3).

$$J_{WT} \frac{d\omega_r}{dt} = T_m - T_e [N.m] \quad (3)$$

Where J_{WT} is the moment of inertia of the WT in kg.m^2 , ω_r is the rotor speed in rad/s, T_m and T_e are the mechanical and electromagnetic torque respectively in Newton-meter (N.m). Usually, the parameters

employed in dynamic stability studies use the inertial constant (H) instead of J , which is defined as the ratio between the kinetic energy stored in the rotating mass and the rated power of the WT. Generally, in power systems, typical values of H vary between 2 s and 9 s (4).

$$H = \frac{\frac{1}{2}J_{WT}\omega_0^2}{S_{rated}} [\text{s}] \quad (4)$$

Where ω_0 is the rated speed of the WT in rad/s, and S_{rated} is the rated power in VA. The quotient between ω_r and ω_0 is the rotor speed in pu as in (5).

$$\omega_{rot} = \frac{\omega_r}{\omega_0} [pu] \quad (5)$$

Considering that the product between the torque and the rotor speed is the rotor power, and replacing (4) and (5) in (3), the differential of the WT is obtained as (6).

$$2H\omega_{rot} \frac{d\omega_{rot}}{dt} = P_{inertia} [pu] \quad (6)$$

The (6) describes the inertia power component of a WT, obtained from the rotor speed and the inertia constant. However, full-scale converter WTs decouple the inertial response of the rotor from the power system. This is accomplished by the speed regulator of the WT, which sets the reference power to the electronic converter. Based on this, it is possible to set another value of the inertial power component, by employing the system frequency measured at the point of common coupling of the WT (f), and a virtual inertia constant (H_v). Analogously to (6) a new inertial power component is defined in (7).

$$2H_v f \frac{df}{dt} = P_{inertia}' [pu] \quad (7)$$

Thus, the general expression of the power flow of WTs that participate in the frequency control can be obtained as (8).

$$P_{WT} = P_{OP} - 2H_v f \frac{df}{dt} + k_D(f_0 - f) + \frac{(f_0 - f)}{R} [pu] \quad (8)$$

Where P_{OP} is the optimal power of the WT, obtained from the tracking characteristic curve [7], [8]. From (8), different works have been developed. The papers presented in [9], [10] propose a droop control system, which is activated in case the frequency of the system exceeds the dead band of the frequency regulator (FR). The research carried out in [11], [12] suggests the use of a damping control scheme, with the purpose of mitigating oscillations in the power system. On the other hand, the recent papers presented in [13]-[16] propose an inertial control scheme with the purpose of attenuating the frequency variation at the beginning of the disturbance. In other words, the WT provides the instantaneous reserve to the power system.

Some research suggests combining two or more control methodologies discussed above. As an example, the combination of control droop, control damping, and the reduction of the output power of the WT. This scheme corresponds to the primary frequency control, which is treated in the works [17]-[19]. In summary, as (9).

$$P_{WT,PFC} = P_{sched} + k_D(f_0 - f) + \frac{(f_0 - f)}{R} [pu] \quad (9)$$

Where P_{sched} is the scheduled output power of the WT, which is always less than P_{OP} to set the required generation reserve. For instance, in [18] the generation reserve is obtained by adjusting the pitch angle of the WT; consequently, the WT operates at a non-optimal operating point. In a power system with a high level of wind penetration, the reduction of wind generation causes the dispatch of thermal power plants since it is necessary to cover the same energy demand. This control scheme is opposed to the postulates enunciated in the introduction; that is, the reduction of wind power produces greater pollution and the depletion of fossil fuels. For this reason, this scheme will not be treated in the present work.

The papers published in [20]-[23] employ all the terms described in equation 8; namely, the WT behaves like a virtual synchronous generator (VSG). This constitutes the current research trend for WTs to participate in the frequency control of the power system. The concept of VSG is to emulate the behavior of a synchronous machine, or a particular characteristic of it. This concept is not only limited to wind generation applications, but also in other renewable generation systems that have stored energy, or in applications that involve energy storage systems (ESS). Unlike the works cited above, which obtain the generation reserve by

reducing the output power of the wind turbine or by using ESS, this work proposes to take advantage of the energy stored in the inertia of the rotating mass of the WT by means of a change in its control system. This topic is addressed in the next chapter and constitutes the main contribution of this work.

3. A NOVEL CONTROL SYSTEM FOR THE WIND TURBINE

According to the previous section, in this work, the VSG concept is proposed for the WT. In order to achieve that goal, the FR has to incorporate the three control loops defined in section 2: droop control, damping control, and inertia control. Additionally, during normal operation, the WT must operate at the point of maximum efficiency. For this reason, the output power of the WT is not reduced, so the generation reserve is obtained from the energy stored in the rotating mass of the rotor.

Under these premises, the performance of the WT for frequency regulation varies according to the output power, the stored energy, and the parameters of the FR. This means that a set of specific values of the FR at high wind speeds may not be optimal for low wind speeds and vice versa. This is due to the non-linearity between the rotor speed, the power generated by the WT, and the energy stored in the rotor. This problem has not been addressed in the literature, and it is proposed to be resolved, being the main contribution of this work.

In this work, an adaptive control strategy is proposed as a solution to the problem of nonlinearity of the WT. The adaptation is the mechanism by which the controller is able to change its parameters to respond to a change in the operating conditions of the WT (rotor speed). According to Figure 1, the control system developed has the typical tracking characteristic curve and the adaptive gain scheduling control system (AGSCS). The AGSCS is composed of the FR and a fuzzy inference system (FIS), which calculates the parameters of the FR. In the case there are no frequency disturbances, the FR is deactivated, and the value of P_{FC} is zero. Therefore, the power reference of the WT ($P_{WT,ref}$) is equal to the power optimal point (P_{OP}) of the tracking characteristic curve. In this way, the WT presents the typical dynamic behavior. Due the controller uses the kinetic energy stored in the rotor; it is convenient to estimate the energy stored as a function of the WT rotor speed. This is discussed in the next section.

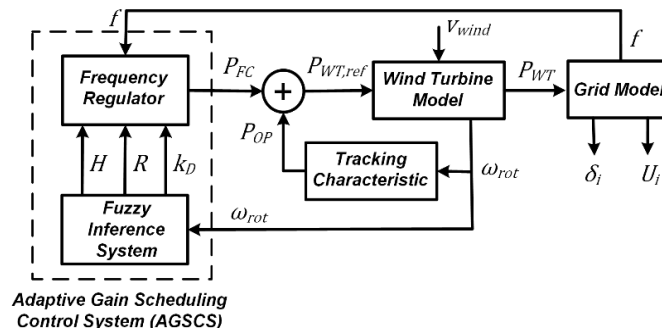


Figure 1. Model of the wind turbine with the AGSCS

3.1. Energy storage capacity of the wind turbine

The use of the WT as an ESS to provide power during frequency regulation requires the estimation of its storage capacity. This is carried out by means of dynamic simulations that allow estimating the energy stored in the inertia of the rotor. The principle of energy storage is carried out in the following way: when it is necessary to increase the wind power injected into the network, the process is carried out by decelerating the rotor, which produces a decrease in the kinetic energy of the rotating mass of the WT. On the other hand, when it is necessary to decrease the power, the process is carried out by accelerating the rotor, producing an increase in the kinetic energy stored in the rotating mass of the WT. Namely, during frequency regulation, the operating principle of the variable speed WT is similar to a flywheel ESS [2]. The energy stored in the rotating mass of the WT is directly proportional to the moment of inertia of the turbine-generator set J_{WT} ($J_T + J_G$) and the square of the rotation speed ω_r . Therefore, the variations of the rotor speed produce increases or decreases in the kinetic energy of rotation. This can be calculated as (10).

$$\Delta E_{WT} = \frac{1}{2} J_{WT} \Delta \omega_r^2 = k_1 \Delta \omega_r^2 \quad (10)$$

Where, ΔE_{WT} is the variation of the kinetic energy of the rotor, and k_1 is constant. In this sense, the energy analysis is carried out by numerical calculation through dynamic simulations. The maximum power point

tracking (MPPT) of the WT is modified, applying positive power steps ($+\Delta P_{mec}$) and negative power steps ($-\Delta P_{mec}$). Due to the non-linearity between wind speed (v_{wind}) and the mechanical power produced (P_{mec}), the magnitude of the power step is limited to 10% of the reference power defined by the MPPT (linearization of nonlinear systems around an operating point). Then, the positive power step and the time (ΔE_{WT}) required for the WT to decelerate to its minimum rotor speed ($\omega_{r,Min} = 0.5$) are registered. Analogously, the values of negative power steps and the time required for the WT to saturate ($\omega_{r,Max} = 1.0$) are recorded. Based on the variations in power and the associated times to reach the minimum and maximum speed of operation of the WT, the energy that can be stored or extracted from the rotating mass of the WT is determined with (11).

$$\Delta E_{WT} = \Delta P_{mec} \Delta t_{WT} \text{ [J]} \quad (11)$$

The results obtained for the detailed model of a 2 MW type 4 WT that is part of the Simulink® software library [24] are shown in Table 1. Note that the rotor speed and the state-of-charge (SOC) are used indistinctively in the second column of Table 1; where $SOC = 0.5$ corresponds to the minimum load of the WT ($P_{mec} = 0.064$ pu); and at $SOC = 1.0$, the WT is at full load ($P_{mec} = 1.0$ pu).

It is important to note that as the rotor speed increases, the time available to supply reserve power decreases. It is possible to find an explanation for this phenomenon by means of the analytical study of the equations that describe the static behavior of the WT. In this sense, the mechanical power of a WT (P_{mec}) can be found with (12).

$$P_{mec} = \frac{1}{2} \rho A v_{wind}^3 C_p(\lambda, \beta) \text{ [W]} \quad (12)$$

Where ρ is the air density (1.225 kg/m^3), A is the rotor area (m^2), v_{wind} is the wind speed (m/s), λ is the tip speed ratio, β is the pitch angle, and $C_p(\lambda, \beta)$ is the power coefficient of the WT, which describes the fraction of the wind power that is converted by the turbine into mechanical power. The value of λ can be found as (13).

$$\lambda = \frac{\omega_r R_{rot}}{v_{wind}} \quad (13)$$

Where R_{rot} is the rotor radius. Considering that the WT operates near the MPPT, the values of λ and C_p remain constant [25]. Replacing (13) in (12), obtained (14) and (15).

$$P_{mec} = \frac{1}{2} \rho A C_p(\lambda, \beta) \left(\frac{\omega_r R_{rot}}{\lambda} \right)^3 \text{ [W]} \quad (14)$$

$$\Delta P_{mec} = k_2 \Delta \omega_r^3 \text{ [W]} \quad (15)$$

Where k_2 is constant. The time of loading/unloading of the WT can be found employing (10), (11), and (15).

$$\Delta t_{WT} = \frac{\Delta E_{WT}}{\Delta P_{mec}} = \frac{k_1}{k_2 \Delta \omega_r} \text{ [s]} \quad (16)$$

The (16) denotes that for high variations in rotor speeds produce shorter times for the WT to saturate or exhaust its stored energy. As an advantage, the output power of the WT is proportional to the cube of the rotor speed. These considerations must be considered in the design of the controller responsible for monitoring the state of charge of the WT. This aspect is addressed in the next section.

Table 1. Loading and unloading capacity of the WT

Operating point of the WT				Unload		Load	
v_{wind} [m/s]	$\omega_{rot} = SOC$ [pu]	P_{mec} [MW]	ΔP_{mec} [MW]	Δt_{WT1} [s]	E_{WT1} [MJ]	Δt_{WT2} [s]	E_{WT2} [MJ]
5	0.5	0.128	± 0.0128	0	0	1290	16.51
6	0.555	0.234	± 0.0234	60	1.40	671	15.70
7	0.626	0.374	± 0.0374	43	1.61	396	14.81
8	0.713	0.56	± 0.056	36	2.02	183	10.25
9	0.809	0.8	± 0.08	33	2.64	78	6.24
10	0.907	1.098	± 0.1098	30	3.29	17	1.87
11	0.984	1.468	± 0.1468	22	3.23	2	0.29

3.2. Frequency regulator

The frequency control scheme is based on the standard model employed in speed regulators of thermal turbines, which is displayed in Figure 2(a). The FR is composed of two parts: the lower control loop defined by (1) and (2), and the higher control loop that synthesizes the inertial response (7). In case the

frequency of the power system varies from the reference value f_0 , the FR calculates the value of the three power components defined in (1), (2), and (6). These power components depend on the parameters H_v , R and k_D ; which are calculated by the fuzzy inference system.

3.3. Fuzzy inference system

The aim of the fuzzy inference system, for high rotor speeds, is to maximize the use of the kinetic energy stored in the WT. For medium rotor speeds, the fuzzy system prioritizes the stable operation of the WT; this leads to a less utilization of the stored kinetic energy. For low rotor speeds, the energy stored is minimal and the FIS disables the FR. According to Figure 2(b), the FIS is composed of three sub-systems: a fuzzification stage, an inference engine, and a defuzzification stage. The input variable to the FIS is the rotor speed ω_{rot} , which varies between 0 and 1 pu. Therefore, the membership function of the Fuzzification Stage is set in the aforementioned interval. Different membership functions have been evaluated, such as gaussian, trapezoidal and triangular. According to the results obtained, the trapezoidal function is the best option, thus it is chosen in the present work.

As reported by Table 1, if the rotor speed is 0.5 pu, the power of the WT is minimal (0.064 pu), and the energy available for unloading is zero (E_{WT}). Thus, the membership function sets the threshold at 0.51 pu for low rotor speed. Then, the fuzzy variables are defined as follows: $l = 1$, $m = h = 0$. If the rotor speed varies between 0.55 pu and 0.7 pu, the energy stored in the WT is in the range of 1.4 MJ to 2.0 MJ. Therefore, the fuzzification stage sets this interval as medium rotor speed, due there is enough energy stored to perform frequency regulation. The fuzzy variables are $m = 1$, $l = h = 0$. On the other hand, if the rotor speed is greater than 0.8 pu, the energy available for unloading is in the range of 2.6 MJ to 3.3 MJ, thus there is plenty energy to carry out the frequency regulation. Therefore, the membership function sets the rotor speed as high. The fuzzy variables are $h = 1$, $l = m = 0$. For the intermediate intervals: 0.51-0.55 pu and 0.7-0.8 pu, the trapezoidal membership functions take the form of two linear functions, one with a positive slope and the other with a negative slope. Within the range, the sum of these lineal functions is equal to 1.0 pu; namely: $l + m = 1$ and $m + h = 1$.

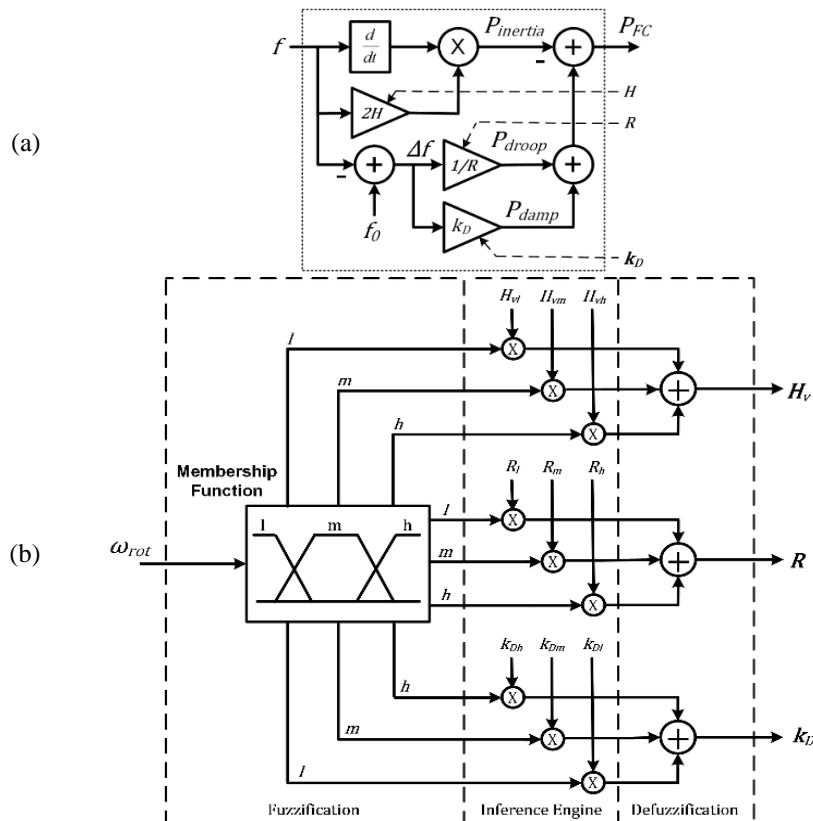


Figure 2. Control system of the wind turbine: (a) FR and (b) FIS

In the inference engine, the fuzzy variables l , m , and h are multiplied by the parameters of the FR. In that sense, it has been defined three values of the parameters R , H_v , and k_D . For low rotor speeds, it is adopted $R_l = \inf$, $H_{vl} = 0$, and $k_{Dl} = 0$. For medium rotor speed: $R_m = 0.05$, $H_{vm} = 2$, and $k_{Dm} = 100$. For high rotor speed,

$R_h = 0.03$, $H_{vh} = 9$ and $k_{Dh} = 200$. The values of R and H_v have been adopted according to the typical parameters of synchronous machines. On the other hand, the value of k_D has been obtained through dynamic simulations using the trial-and-error method. In the stage of defuzzification, the parameters of the FR are obtained, considering that for any value of ω_r , the sum of the fuzzy variables is equal to 1.0 pu.

4. TEST SYSTEM

The 230 kV test system is shown in Figure 3. This model is based on the IEEE 9-bus modified test system which consists of 2 synchronous machines with IEEE type-1 exciters. At bus 2, it is connected a 600 MW steam turbine, at Bus 3 it is connected a 200 MW hydraulic power plant, while at bus 1 it is connected a 270 MW wind farm. In total, there are 9 buses, 6 transmission lines, 3 transformers and 3 constant P-Q loads.

The wind farm consists of 135 variable speed WTs (type 4), the maximum power of each WT is 2 MW if the wind speed is 13 m/s. The cut-in wind speed is 5 m/s, and the cut-out wind speed is 25 m/s. The rotor speed varies between 0.75 rad/s and 1.5 rad/s; if the base rotor speed is 1.5 rad/s, then the rotor speed varies between 0.5 and 1.0 pu. For rotor speeds less than 0.5 pu, the WT is disconnected. The models of the Type 4 WT and the wind speed were developed in [25]-[27].

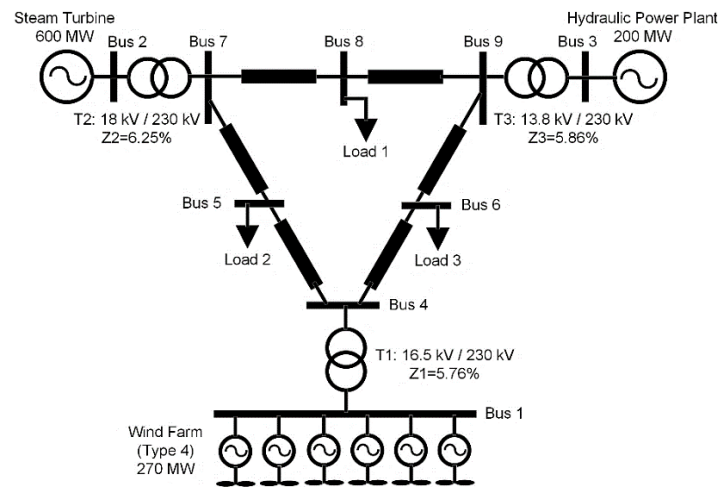


Figure 3. Test system

5. SIMULATION RESULTS

The simulations were carried out considering 3 load conditions, each of them with a different wind speed: low wind speed (6 m/s), medium wind speed (9 m/s) and high wind speed (11 m/s). Table 2 summarizes the dispatches of the test system; the values reported in loads are approximate and include losses in lines and transformers. Regarding the power factor, a value of 0.97 was adopted (lagging). In all cases, the turbine speed is modified by adjusting the FR power P_{FC} , Figures 1 and 2(a).

5.1. Case A: low wind speed

In this case, the wind speed is set constant at 6 m/s, the wind farm produces 32.01 MW and the WP is 4.39 %. It is important to note that wind turbulence has not been considered to facilitate the analysis of the inertial response of the wind farm. Due to the frequency variations caused by renewable generation are minimal, the parameter k_D is set to zero. At time $t = 40$ s, Load 1 increases by 60 MW; this produces an imbalance between generation and demand with the consequent decrease in the frequency of the system as shown in Figure 4(a).

According to Figure 4(a), the wind farm enhances the transient response of the power system if the AGSCS is activated. According to the initial value of ω_{rot} , the parameters of the FR are: $H_v = 2$, $k_D = 0$ and $R = 0.05$ (case 2). In this case, the minimum frequency is 59.62 Hz. If the AGSCS is deactivated (case 1), the minimum frequency is 59.28 Hz. If the FIS is deactivated, and the FR is activated with $H_v = 9$, $R = 0.03$, $k_D = 0$ (case 3), the minimum frequency is 58.33 Hz.

Figure 4(b) shows the rotor speed of the wind farm, it keeps steady at 0.5573 pu if the AGSCS is deactivated (case 1). When the AGSCS is activated (case 2), the rotor speed decreases to 0.5013 pu then recovers to its previous state (0.5573 pu). This allows the wind farm to increase its output power to compensate the load imbalance (Figure 4(c)). If the FIS is deactivated, and the FR is activated with $H_v = 9$, R

$= 0.03$, $k_D = 0$ (case 3), at $t = 45$ s the rotor speed drops below 0.5 and the wind farm is disconnected, so the power output is zero shown in Figure 4(c). This leads to a severe disturbance because the steam turbine and the hydroelectric power plant cover the power shortage, further accentuating the frequency excursion as shown in Figure 4(a), case 3).

The output power of the steam turbine and the hydroelectric power plant is illustrated in Figures 4(d) and 4(e). Comparing case 1 with case 2, it is clearly shown that the AGSCS reduces the dynamic stresses of conventional generators. If the FIS is deactivated, and the FR is activated (case 3) it is observed that the Steam Turbine reaches its rated power at $t = 60$ s, so the hydroelectric power plant must cover the power shortage with a slow transient response shown in Figure 4(e), case 3. Therefore, for low wind speed, case 2 is the best option (AGSCS activated).

Table 2. Dispatches of the test system

Wind speed [m/s]	Wind farm [MW]	Steam turbine [MW]	Hydro power [MW]	Load 1 [MW]	Load 2 [MW]	Load 3 [MW]	Total load [MW]	WP [%]
6	32.0	516.7	179.5	250	215	263.2	728.2	4.39
9	109.7	516.2	179.5	250	300	255.3	805.3	13.6
11	208.8	515	179.4	250	300	353.2	903.2	23.1

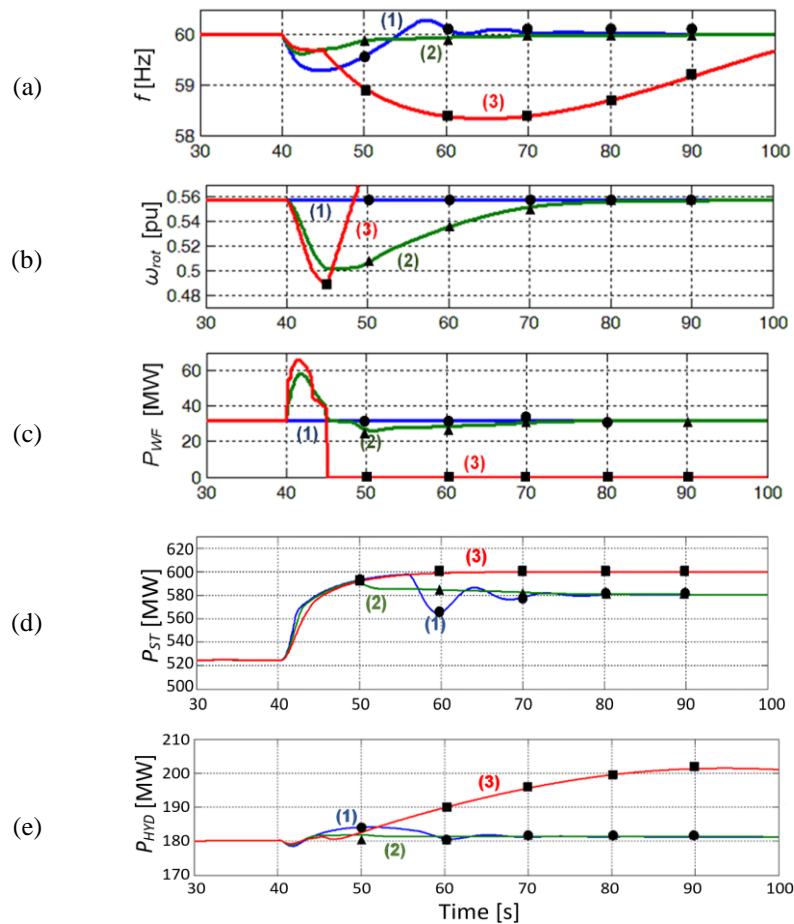


Figure 4. Dynamic response of the test system for low WP: (a) frequency, (b) rotor speed of the WTs, (c) wind farm power output, (d) steam turbine power output, and (e) hydraulic power plant power output. (1●) AGSCS deactivated, (2▲) AGSCS activated, (3■) FIS deactivated, and FR activated ($H_v = 9$, $R = 0.03$, $k_D = 0$)

5.2. Case B: medium wind speed

In this case, the wind speed is 9 m/s, and the wind farm generates 109.68 MW, thereby the WP is 13.62%. Similar to the previous example, the turbulence of the wind has not been considered in order to highlight the inertial response of the wind farm; therefore, the parameter k_D is set to zero. At time $t = 40$ s, Load 1 increases from 250 MW to 310 MW, which produces a decrease in the frequency due to the imbalance between generation and demand shown in Figure 5(a).

Figure 5(a) shows that the AGSCS enhances the transient response of the test system. For case 1 (AGSCS deactivated), the minimum frequency is 59.3 Hz and the rotor speed remains constant at 0.8134 pu Figure 5(b). For case 2, the AGSCS sets the parameters of the FR at $H_v = 9$, $R = 0.03$, $k_D = 0$; this leads to a minimum frequency of 59.71 Hz and ω_r at 0.7539 pu. If the FIS is deactivated, and the FR is activated with $H_v = 2$, $R = 0.5$, $k_D = 0$ (case 3); the minimum frequency is 59.62 Hz and the lowest ω_r is 0.7729 pu. This shows that for higher values of the parameters H_v and R , a greater use of the energy stored in the rotating masses of WTs is made, as shown in Figures 5(b) and 5(c), and a better transient response of the test system is obtained. This simulation and the previous one demonstrate that the FIS chooses the best parameters for the FR.

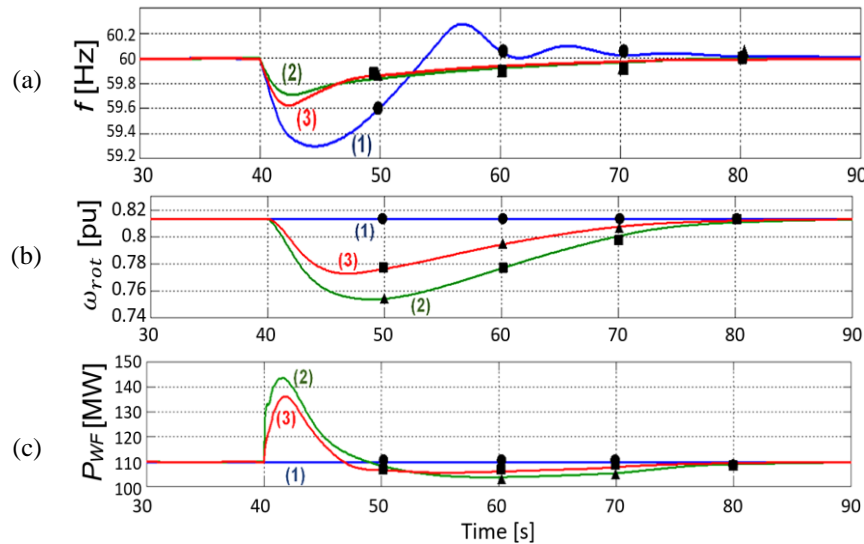


Figure 5. Dynamic response of the test system for medium WP: (a) frequency; (b) rotor speed of the WTs; and (c) wind farm power output, (1●) AGSCS deactivated, (2▲) AGSCS activated, (3■) FIS deactivated, and FR activated ($H_v = 2$, $R = 0.05$, $k_D = 0$)

5.3. Case C: high wind speed

In this simulation, the average wind speed is 11 m/s, the wind farm produces 208.8 MW, and the WP is 23.11%. The turbulent component of the wind speed has been simulated, and the wind speed equivalent model for the wind farm considers the aggregation phenomena. These models are obtained from [26], [27], and the results are shown in Figure 6(a) (see Appendix).

Figures 6(a)-6(c) show case 1 (AGSCS deactivated), case 2 (AGSCS activated), and case 3 (FIS deactivated and FR activated with $H_v = 2$, $R = 0.05$, $k_D = 100$). Clearly, the AGSCS enhances the transient response of the test system, which sets the parameters of the FR at $H_v = 9$, $R = 0.03$, and $k_D = 200$. In particular, the increase of the k_D parameter allows the reduction of the frequency excursion (Figure 6(b)), at the expense of a major utilization of the energy stored in the inertia of WTs' rotational masses, shown in Figure 6(c).

The active power generated in the test system is shown in Figures 6(d)- 6(f). Clearly, it is observed that the AGSCS smooths the power generated by the wind farm (Figure 6(d)) and reduces the mechanical stress of conventional generators, as shown in Figures 6(e) and 6(f). According to Figure 6, the best transient response is obtained when the AGSCS is activated.

6. CONCLUSION

This work presents a novel frequency regulator for wind turbines to improve the transient response of power systems with a high level of wind penetration. Simulations show that the wind farm behavior depends on the operation point, which in turn varies depending on the wind speed. Because it is a non-linear and time-variant system, an AGSCS based on a FIS is required in order to calculate the best parameters of the frequency regulator during the normal and emergency operation. The results show that for low wind speeds, the AGSCS computes low values for the frequency regulator parameters. Although the contribution of reserve power to frequency regulation is low, so is the penetration of wind power. In this case, conventional power plants are the ones that contribute the most to recovering the frequency to its nominal value. As for medium and high wind speeds, the AGSCS calculates high values for the frequency regulator parameters.

This increases the reserve power provided by the wind turbines, helping the power system to restore its nominal frequency faster. Additionally, it is shown that for high levels of wind penetration, turbulent variations in wind speed can cause undesired fluctuations in the system frequency. These variations can be mitigated by adjusting the damping parameter of the frequency regulator; although further studies are required regarding the adjustment of this parameter, since its value depends on the dynamic behavior of the power system under study. Nevertheless, in this case it is demonstrated that the parameters calculated by the AGSCS are the most suitable for performing frequency regulation.

FUNDING INFORMATION

This work was partially financed by the Council for Science and Technology Research (CONICET), the Argentinean National Agency for the Promotion of Science and Technology (ANPCyT) and the National University of San Juan (UNSJ).

AUTHOR CONTRIBUTIONS STATEMENT

This journal uses the Contributor Roles Taxonomy (CRediT) to recognize individual author contributions, reduce authorship disputes, and facilitate collaboration.

Name of Author	C	M	So	Va	Fo	I	R	D	O	E	Vi	Su	P	Fu
Leonardo Javier Ontiveros	✓	✓	✓	✓	✓	✓	✓	✓	✓	✓		✓	✓	✓
Antonio Ernesto Sarasua			✓		✓	✓	✓	✓		✓	✓			✓
Cindy Madrid-Chirinos						✓	✓			✓	✓			

C : Conceptualization

M : Methodology

So : Software

Va : Validation

Fo : Formal analysis

I : Investigation

R : Resources

D : Data Curation

O : Writing - Original Draft

E : Writing - Review & Editing

Vi : Visualization

Su : Supervision

P : Project administration

Fu : Funding acquisition

CONFLICT OF INTEREST STATEMENT

Authors state no conflict of interest.

DATA AVAILABILITY

Derived data supporting the findings of this study are available from the corresponding author, [LO], on request.

REFERENCES

- [1] World Wind Energy Association report, "WWEA Annual Report 2023," *World Wind Energy Association report*. <https://wwindea.org/ss-uploads/media/2024/3/1711538106-40ab83f2-3e01-4c0a-9d28-e0a21bfb72e6.pdf>
- [2] G. O. Suvire and P. E. Mercado, "Active power control of a flywheel energy storage system for wind energy applications," *IET Renewable Power Generation*, vol. 6, no. 1, pp. 9–16, Jan. 2012, doi: 10.1049/iet-rpg.2010.0155.
- [3] S. Guan, X. Yan, G. Cai, and J. Jia, "An active and reactive power coordination control strategy during LVRT period," in *2024 3rd International Conference on Energy, Power and Electrical Technology (ICEPET)*, May 2024, pp. 1759–1763. doi: 10.1109/ICEPET61938.2024.10627099.
- [4] M. Gustavo and J. Gimenez, "Technical and regulatory exigencies for grid connection of wind generation," in *Wind Farm - Technical Regulations, Potential Estimation and Siting Assessment*, InTech, 2011. doi: 10.5772/16474.
- [5] S. Xu, H. Wang, Y. Cao, S. Igarashi, J. Li, and X. Cai, "Inertia response control of self-synchronous voltage source doubly-fed wind turbines in the whole wind speed range," in *2024 IEEE 10th International Power Electronics and Motion Control Conference (IPEMC2024-ECCE Asia)*, May 2024, pp. 151–156. doi: 10.1109/IPEMC-ECCEAsia60879.2024.10567551.
- [6] Z. Zhu, S. Du, L. Zhang, and Q. Qi, "A new coordinated control strategy to improve the frequency stability of microgrid based on de-loaded capacity of wind turbine," in *2020 5th Asia Conference on Power and Electrical Engineering (ACPEE)*, Jun. 2020, pp. 645–651. doi: 10.1109/ACPEE48638.2020.9136560.
- [7] W. Yan, X. Wang, W. Gao, and V. Gevorgian, "Electro-mechanical modeling of wind turbine and energy storage systems with enhanced inertial response," *Journal of Modern Power Systems and Clean Energy*, vol. 8, no. 5, pp. 820–830, 2020, doi: 10.35833/MPCE.2020.000272.
- [8] M. H. Ravanji and M. Parniani, "Small-signal stability analysis of DFIG-based wind turbines equipped with auxiliary control systems under variable wind speed," in *2020 IEEE International Conference on Environment and Electrical Engineering and 2020 IEEE Industrial and Commercial Power Systems Europe (EEEIC/I&CPS Europe)*, Jun. 2020, pp. 1–7. doi: 10.1109/EEEIC/ICPSEurope49358.2020.9160721.

- [9] Y. Zhang, J. Duan, J. Tao, Z. Li, and L. Li, "Fuzzy droop control strategy for doubly-fed wind turbines considering frequency influencing factors," in *2024 6th Asia Energy and Electrical Engineering Symposium (AEEES)*, Mar. 2024, pp. 529–533. doi: 10.1109/AEEES61147.2024.10544770.
- [10] W. Chen, T. Zheng, H. Nian, D. Yang, W. Yang, and H. Geng, "Multi-objective adaptive inertia and droop control method of wind turbine generators," *IEEE Transactions on Industry Applications*, vol. 59, no. 6, pp. 7789–7799, 2023, doi: 10.1109/TIA.2023.3307368.
- [11] Z. Li, Z. Ma, C. Yi, X. Cheng, Y. Zhang, and X. Zhang, "Study on oscillation of doubly fed wind turbine based on additional damping control strategy," in *2022 5th Asia Conference on Energy and Electrical Engineering (ACEEE)*, Jul. 2022, pp. 79–84. doi: 10.1109/ACEEE56193.2022.9851824.
- [12] K. Gunther and C. Sourkounis, "Active damping control for variable-speed wind turbines with VSM as grid-side control," in *2021 22nd IEEE International Conference on Industrial Technology (ICIT)*, 2021, pp. 304–309, doi: 10.1109/ICIT46573.2021.9453518.
- [13] R. Azizpanah-Abarghoee, M. Malekpour, T. Dragicevic, F. Blaabjerg, and V. Terzija, "A linear inertial response emulation for variable speed wind turbines," *IEEE Transactions on Power Systems*, vol. 35, no. 2, pp. 1198–1208, Mar. 2020, doi: 10.1109/TPWRS.2019.2939411.
- [14] C. Nikolakakos, U. Mushtaq, P. Palensky, and M. Cvetkovic, "Improving frequency stability with inertial and primary frequency response via dfig wind turbines equipped with energy storage system," in *2020 IEEE PES Innovative Smart Grid Technologies Europe (ISGT-Europe)*, Oct. 2020, pp. 1156–1160. doi: 10.1109/ISGT-Europe47291.2020.9248807.
- [15] C. Wang, C. Li, K. Zeng, Y. Chen, L. Xiao, and C. Sun, "Research of inertial control strategy of wind turbines under low frequency situation of hydro-dominated system," in *2021 IEEE 4th International Electrical and Energy Conference (CIEEC)*, May 2021, pp. 1–6, doi: 10.1109/CIEEC50170.2021.9510587.
- [16] J. C. Martinez, S. A. Gomez, J. L. Rodriguez Amenado, and J. Alonso-Martinez, "Analysis of the frequency response of wind turbines with virtual inertia control," in *2020 IEEE International Conference on Environment and Electrical Engineering and 2020 IEEE Industrial and Commercial Power Systems Europe (EEEIC/I&CPS Europe)*, 2020, pp. 1–6, doi: 10.1109/EEEIC/ICPSEurope49358.2020.9160718.
- [17] C. Xiu, Z. Lv, Z. Zhou, J. Wang, and Y. Guo, "Deloading control strategy of permanent magnet direct drive wind turbine with adaptive droop gain," in *2024 IEEE 7th International Electrical and Energy Conference (CIEEC)*, May 2024, pp. 5058–5063. doi: 10.1109/CIEEC60922.2024.10583672.
- [18] B. Lu, G. Zhu, C. Zhang, L. Ding, S. Wang, and Y. Guan, "Pitch deloading method of wind farm for optimal frequency control performance," in *2023 6th International Conference on Energy, Electrical and Power Engineering (CEEPE)*, May 2023, pp. 344–349. doi: 10.1109/CEEPE58418.2023.10166677.
- [19] W. Bao, L. Ding, Y. C. Kang, and L. Sun, "Closed-loop synthetic inertia control for wind turbine generators in association with slightly over-speeded deloading operation," *IEEE Transactions on Power Systems*, vol. 38, no. 6, pp. 5022–5032, Nov. 2023, doi: 10.1109/TPWRS.2022.3224431.
- [20] J. Xi, H. Geng, and X. Zou, "Decoupling scheme for virtual synchronous generator controlled wind farms participating in inertial response," *Journal of Modern Power Systems and Clean Energy*, vol. 9, no. 2, pp. 347–355, 2021, doi: 10.35833/MPCE.2019.000341.
- [21] C. Shao, Z. Li, R. Hao, Z. Qie, G. Xu, and J. Hu, "A wind farm frequency control method based on the frequency regulation ability of wind turbine generators," in *Proceedings - 2020 5th Asia Conference on Power and Electrical Engineering, ACPEE 2020*, 2020, pp. 592–596, doi: 10.1109/ACPEE48638.2020.9136431.
- [22] Q. Meng, Y. Ren, and H. Liu, "Frequency stability analysis of grid-forming PMSG based on virtual synchronous control," *IEEE Access*, vol. 12, pp. 84134–84148, 2024, doi: 10.1109/ACCESS.2024.3414424.
- [23] A. Mishra, A. S. Mir, and N. Prasad Padhy, "Improving system inertial support from PMSG based wind turbines with adaptive inertial and damping control," in *2023 IEEE International Conference on Power Electronics, Smart Grid, and Renewable Energy (PESGRE)*, Dec. 2023, pp. 1–5, doi: 10.1109/PESGRE58662.2023.10404366.
- [24] "Wind Farm - Synchronous generator and full-scale converter (Type 4) average model," *MATLAB/Simulink Website*. <https://www.mathworks.com/help/sps/ug/wind-farm-synchronous-generator-and-full-scale-converter-type-4-detailed-model.html>
- [25] L. J. Ontiveros and P. E. Mercado, "Modeling of variable-speed wind farms for power systems dynamic studies," in *Proc. 14th Ibero-American Regional Meeting of CIGRÉ, Ciudad del Este, Paraguay*, 2011, pp. 1–8.
- [26] L. J. Ontiveros, "Incorporation of redox batteries in wind farms to perform secondary frequency regulation," San Juan National Univ. (UNSJ), 2011.
- [27] L. J. Ontiveros, P. E. Mercado, and G. O. Suvire, "A new model of the double-feed induction generator wind turbine," in *2010 IEEE/PES Transmission and Distribution Conference and Exposition: Latin America (T&D-LA)*, Nov. 2010, pp. 263–269. doi: 10.1109/TDC-LA.2010.5762892.

APPENDIX

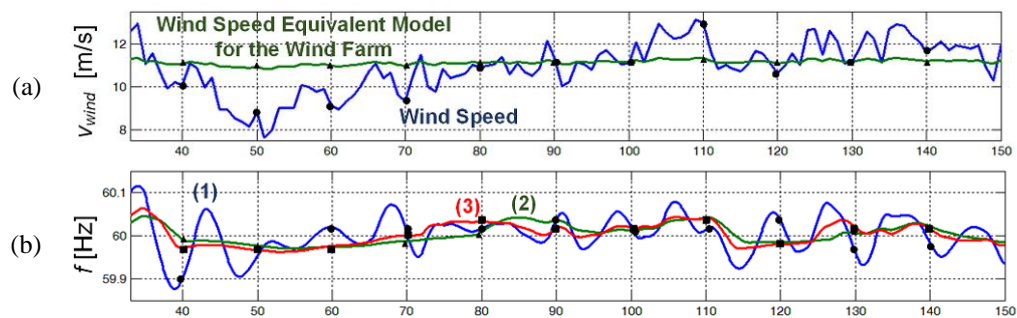


Figure 6. Dynamic response of the test system for high WP: (a) wind speed models; (b) system frequency

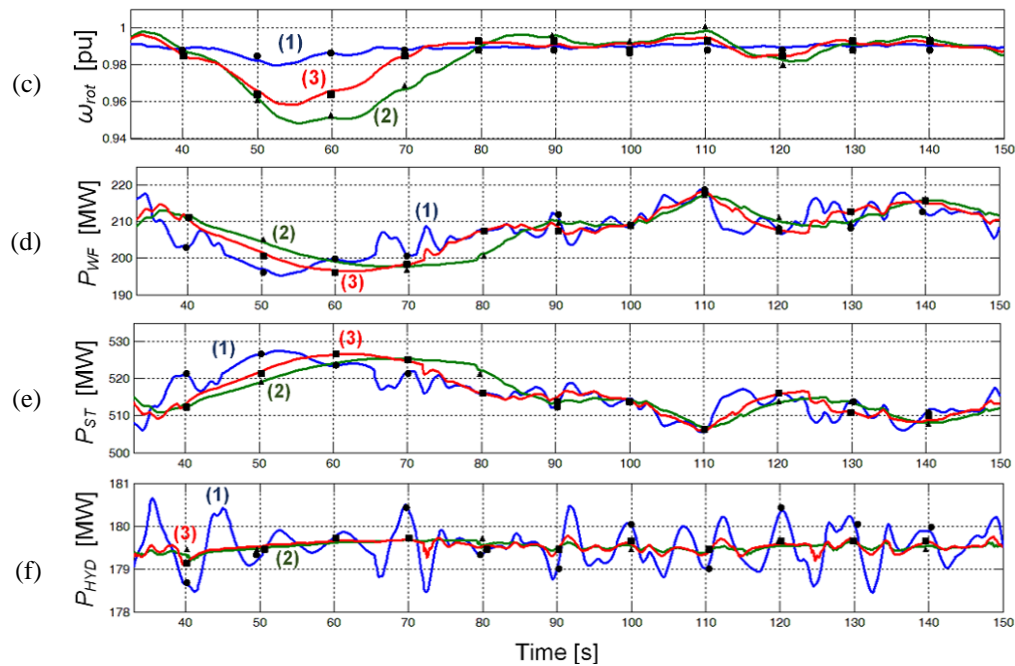








Figure 6. Dynamic response of the test system for high WP: (c) rotor speed of the WTs; (d) wind farm power output; (e) steam turbine power output; and (f) hydraulic power plant power output (1●) AGSCS deactivated; (2▲) AGSCS activated; (3■) FIS deactivated, and FR activated ($H_v = 2$, $R = 0.05$, $k_D = 100$) (continued)

BIOGRAPHIES OF AUTHORS






Leonardo Javier Ontiveros    was born in San Juan, Argentina, on October 9, 1977. He graduated as an electronic engineer from the UNSJ, Argentina, in 2004. He received his Ph.D. from the same University in 2011, carrying out part in the COPPE institute, in the Federal University of Rio de Janeiro in Brazil. Dr. Ontiveros is currently a professor of electrical engineering at the UNSJ and a researcher with CONICET. His research interests include simulation methods, power systems dynamics and control, power electronics modeling and design, and the application of wind energy and energy storage in power systems. He can be contacted at email: lontiveros@iee-unsjconicet.org.



Antonio Ernesto Sarasua    was born in San Juan, Argentina. He graduated as an Electrical Engineering from the National University of San Juan (UNSJ), Argentina in 1994, and received the Ph.D. degree from the UNSJ in 2005. Since 2006, Dr. Sarasua is Professor at the Instituto de Energía Eléctrica – CONICET-UNSJ. His research interests include power system stability and bifurcation, simulation methods and the application of energy storage in power systems. He can be contacted at email: asarasua@iee-unsjconicet.org.



Cindy Madrid-Chirinos    received the B.Eng. degree in chemical and electrical engineering in National University of Honduras in 2011 and 2012 respectively, and currently student of M.Eng. degree in Electrical Engineering from National University of San Juan, Argentina. Her research interests include the field of electrical power systems, photovoltaic power systems, harmonics, remote sensing data analysis via geospatial technologies, and batteries implemented in power system. She can be contacted at email: cmadrid@iee.unsj.edu.ar.